

Pax3 induces cell aggregation and regulates phenotypic mesenchymal-epithelial interconversion

O'Neil Wiggan¹, Marc P. Fadel² and Paul A. Hamel^{1,*}

¹Department of Laboratory Medicine and Pathobiology, and ²Department of Anatomy and Cell Biology, Faculty of Medicine, University of Toronto, Toronto, Ontario, M5S 1A8 Canada

*Author for correspondence (e-mail: paul.hamel@utoronto.ca)

Accepted 26 October 2001

Journal of Cell Science 115, 517-529 (2002) © The Company of Biologists Ltd

Summary

Paired box-containing transcription factors play fundamental roles in pattern formation during embryonic development of diverse organisms ranging from *Drosophila* to mammals. Although mutations to *Pax3* and other Pax-family genes in both mice and humans result in numerous tissue-specific morphological defects, little is known about the cellular processes that Pax genes regulate. We show that ectopic *Pax3* expression in two distinct phenotypically mesenchymal mammalian cell lines induces the formation of multi-layered condensed cell aggregates with epithelial characteristics. For one of these lines, we showed further that *Pax3*-induced cell aggregation is accompanied by specific morphological changes, including a significant reduction in cell size, altered cell shape and dramatic

alterations to both membrane and cytoskeleton architecture. In addition to mediating a phenotypic mesenchymal-to-epithelial transition, *Pax3* also establishes the conditions in these cells for a subsequent hepatocyte growth factor/scatter factor (HGF/SF)-induced phenotypic epithelial-to-mesenchymal transition. Thus, our data show a novel morphogenetic activity for *Pax3* which, when absent in vivo, is predicted to give rise to the observed structural defects in somites and the neural tube during embryonic development.

Key words: Pax3, Mesenchymal-epithelial transition, Cell aggregation, Cell adhesion, c-met

Introduction

In a theoretical model of morphogenesis, Atchley and Hall (Atchley and Hall, 1991) proposed cell condensation, the aggregation of like cells, as the basic unit from which morphology is constructed during development. Indeed, cell condensation is an early developmental process in essentially every organ during vertebrate embryogenesis (Thesleff et al., 1995). Likewise, transformations between the two major phenotypic cell types, epithelial and mesenchymal, play an important role in the genesis and patterning of numerous tissues and organs during development (Hay, 1995). Mesenchymal condensation and mesenchymal-to-epithelial transformations play pivotal roles in the formation and patterning of, for example, somitic (Christ and Ordahl, 1995) and kidney (Davies, 1996) structures.

Aborted organogenesis at the point of mesenchymal condensation or cell aggregation is a feature common to mice with mutations in distinct Pax genes (Dahl et al., 1997). The Pax-family genes encode a class of transcription factors that are essential for normal embryonic development. Originally identified as regulators of pattern formation during *Drosophila* embryogenesis, nine different Pax genes have been identified in mammals, *Pax1* to *Pax9* (Walther et al., 1991), all of which encode proteins containing a DNA-binding motif termed the paired box (Noll, 1993). Analyses of animals harboring naturally occurring or targeted mutations of different Pax genes revealed their fundamental requirement for orchestrating proper morphological development of various tissues and organs (Dahl et al., 1997). Some of the many examples include *Pax3* mutant mice, where maintenance of epithelial aggregation in somitic

cells of the dermomyotome is lost (Daston et al., 1996), and *Pax2* mutant mice, in which aborted kidney development occurs due to the failure of the metanephric mesenchyme to condense and undergo epithelial transformation (Torres et al., 1995). For these mutant animals, a role for Pax proteins in regulating cell aggregation/mesenchymal condensation and/or mesenchymal-to-epithelial transformation has been implied.

During mouse embryogenesis, *Pax3* is expressed in several developing tissues including the brain, dorsally throughout the neural tube, in neural crest cells, the dermomyotome and in migratory somitic muscle precursors (Goulding et al., 1991). Mutations to *Pax3* in mice results in the splotch (*sp*) phenotype (Epstein et al., 1991). Homozygous mutant *sp* embryos exhibit a number of developmental defects including impaired neural tube closure, absence of limb muscles, persistent truncus arteriosus and defects to many neural crest-derived structures (Auerbach, 1954; Franz, 1989; Franz et al., 1993). In humans, heterozygous mutations to *Pax3* cause Waardenburg syndrome, which is characterized by pigmentation, and hearing and facio-skeletal anomalies (Baldwin et al., 1992; Tassabehji et al., 1992). Recent studies have begun to provide insights into the cellular and molecular processes that Pax genes may regulate during embryogenesis. During muscle development, for example, *Pax3* appears to regulate the expression of myogenic determination factors (Maroto et al., 1997; Tajbakhsh et al., 1997) as well as migration of muscle precursors via regulation of c-met expression (Daston et al., 1996; Epstein et al., 1996; Yang et al., 1996). However, the cellular and molecular mechanisms by which *Pax3* specifically regulates morphogenesis remains elusive.

We show that ectopic Pax3 expression in osteogenic Saos-2 cells results in the formation of cell aggregates with epithelial characteristics. Ectopic Pax3 expression in Saos-2 cells leads to increased Ca²⁺-dependent cadherin-mediated intercellular adhesion and formation of polarized epithelium. Furthermore, we show that, although Pax3 induces phenotypic epithelialization of these mesenchymal cells, it also induces these cells to become competent to respond to a factor, specifically hepatocyte growth factor/scatter factor (HGF/SF), that reverts the epithelial phenotype. Our results reveal a novel activity for Pax3 and suggest a mechanism by which Pax genes may regulate pattern formation during development.

Materials and Methods

Plasmids and antibodies

Plasmids for pAdtrack and pAdeasy, as well as BJ5183 bacterial cells, were gifts of B. Vogelstein (Howard Hughes Medical Institute, Baltimore). MDCK cells and the human HGF/SF expression vector were gifts of M. Park (McGill, University, Montreal, PQ, Canada). Monoclonal pan-cadherin antibodies was a gift of M. Opas (University of Toronto, Toronto, ON, Canada). Anti- α -catenin and β -tubulin antibodies were gifts of L. Langille (University of Toronto, Toronto, ON, Canada). Antibodies to β -catenin and ZO-1 were obtained from Transduction Laboratories (Lexington, KY). Anti-flag M2, anti-actin, anti-vinculin and Rhodamine-conjugated phalloidin were obtained from Sigma Chemicals (Oakville, ON, Canada). Anti-h-met (C-28) and anti-cadherin-11/OB-cadherin (E-5) were obtained from Santa Cruz Biotechnology (Santa Cruz, CA). Texas Red conjugated secondary antibodies were obtained from Jackson Immuno Research Laboratories (West Grove, PA).

Cell culture and metabolic labeling

Both human Saos-2 osteosarcoma and Rh30 rhabdomyosarcoma cells were grown in DMEM supplemented with 10% fetal calf serum (Sigma, Oakville, ON, Canada). Saos-2 cells do not express Pax3, determined by western blot analysis of whole-cell lysates (O.W., unpublished). The Rh30 rhabdomyosarcoma expresses a Pax3/FKHR fusion protein, which has been shown previously to exhibit activities distinct from that of Pax3 (Epstein et al., 1998). Metabolic labeling and immunoprecipitations were as previously described (Hinck et al., 1994).

Construction of adenoviruses and infection procedures

Adenoviruses were generated as previously described (He et al., 1998). Briefly, cDNA encoding either β -galactosidase or an amino-terminal flag-epitope tagged mouse Pax3 was subcloned into the pAdtrack vector. pAdtrack constructs were linearized with *PmeI* and co-transformed with pAdeasy into BJ5183 bacterial cells. Recombinant viral DNA was isolated from BJ5183 cells and used to transfect 293 cells to generate replication-deficient infectious adenoviral particles. Viruses were harvested from 293 cells and titered on human C33A cells by counting live green fluorescent protein (GFP)-positive cells at 24 hours postinfection. Viral titers were typically in the range of 1×10^8 – 1×10^9 expression forming units/ml. For infection of Saos-2 or Rh30 cells, typically 1×10^6 cells were plated on 60 mm plates the day before infection. The following day, cells were infected at an m.o.i of 10 in a total of 4 ml of normal media. Media was replenished at 2–3 day intervals.

Immunofluorescence and microscopy

Cells grown on glass coverslips were rinsed in PBS before being fixed in freshly prepared 4% paraformaldehyde for 10 minutes at room temperature. For β -tubulin staining, cells were fixed for 10 minutes in

50% methanol/50% acetone at room temperature. Coverslips were rinsed in PBS and cells were then exposed to a solution of 0.2% Triton X-100 and 3% bovine serum albumin (BSA) in PBS for 30 minutes for permeabilization and to block nonspecific binding. Cells were then incubated for 60 minutes at room temperature with the appropriate primary antibody, diluted in 3% BSA in PBS. Cells were then rinsed briefly 4–5 times with PBS and subsequently incubated with the appropriate Texas Red-conjugated secondary antibody in 3% BSA in PBS for 50 minutes. After four washes with PBS, coverslips were then mounted with vinyl mountant (Opas et al., 1996). For F-Actin staining, cells were incubated with Rhodamine-conjugated phalloidin in 3% BSA in PBS for 50 minutes following permeabilization, rinsed with PBS and then mounted. GFP images were captured on a Zeiss axiophot microscope equipped with a CCD camera. Confocal images were obtained on a Zeiss LSM microscope. Unless otherwise indicated, confocal images represent projections of 10–15 optical sections acquired at 0.4 μ m intervals. For Fig. 7 (I–L), optical sections were acquired at 0.8 μ m intervals. Phase-contrast images were obtained with a Nikon inverted microscope onto Kodak Plus-X pan 125ASA film. Morphometric analysis was performed using Scion Image beta 3b, an adaptation of NIH Image for PC (Scion Corporation, Fredrick, MD) and Image-1 (Universal Imaging, West Chester, Pennsylvania) software. Scanning electron micrographs were obtained on a Hitachi 570 microscope at 15 kV.

RNA isolation and RT-PCR

RNA was isolated using Trizol (Gibco, Burlington, ON, Canada) according to the manufacturer's instructions. DNase treatment of the RNA and cDNA synthesis was done essentially as described previously (Munsterberg et al., 1995). Exceptions were that 2 μ g of RNA was used for cDNA synthesis, and the reverse transcriptase utilized was Superscript II RT (Gibco). For PCR amplification, 1 μ l cDNA was used in a final volume of 50 μ l with 1 unit of Taq polymerase (Gibco). PCR products were amplified for 27 cycles, which was determined to be in the linear range for all three products; 15 μ l of each PCR reaction were analyzed on a 2% agarose gel. Primers for c-met, designed to be degenerate for detection of both human and mouse transcripts, were as follows: 5'-GTG T/CTG GAA CAC CCA GAT TGT T-3', 5'-CAA AGA AA/G TGA TGA ACC GGT CC-3' (nucleotides 265–587). Primers for mouse Pax3 were 5'-CAG GAG ACA GGC TCC ATC CGA-3', 5'-CCT TTC TAG ATC CGC CTC CTC-3' (nucleotides 271–522). Primers for GAPDH were as described (Wang et al., 1997). The expected product sizes are as follows: c-met, 322bp; Pax3, 251bp; GAPDH, 880 bp. PCR products were confirmed by restriction digests. PCR products were quantified using NIH Image software.

HGF experiment

Conditioned media containing HGF/SF was obtained by transfection of COS cells with a cDNA encoding human HGF/SF. Control conditioned media was obtained by transfection with an empty pcDNA3 vector. Conditioned media was harvested at 3 days post-transfection and HGF/SF titer determined in a MDCK scatter assay as described previously (Royal et al., 2000). Saos-2 cells were plated in 12-well plates and infected with control or Ad-Pax3^{flag} viruses at a multiplicity of infection (m.o.i.) of 10. At 3 days postinfection, by which time Ad-Pax3^{flag}-infected cells had formed aggregates, cells were exposed to six scatter units of HGF conditioned media or the equivalent volume of control conditioned media in a total volume of 1 ml. Live cells were analyzed by phase contrast microscopy at various times following HGF treatment for up to 24 hours.

Ca²⁺ switch assay

The Ca²⁺ switch assay was performed as described (Gumbiner et al.,

1988). Briefly, Saos-2 cells were infected with control or Ad-Pax3^{flag} viruses in the presence of normal Ca²⁺-containing media. At 3 days postinfection the media was replaced with low Ca²⁺-containing medium. Live cells were subsequently examined at various times up to 24 hours by phase contrast microscopy.

Western immunoblots and cell fractionation

For cell fractionation, cells were washed with cold PBS and then scraped into lysis buffer (10 mM Tris.HCl (pH 8.0), 120 mM NaCl, 1% NP-40) plus a cocktail of protease inhibitors. Lysates were vortexed and incubated at 4°C for 15 minutes followed by centrifugation at 17,000 *g* for 15 minutes at 4°C. The supernatant (soluble fraction) was recovered and the pellet, representing the insoluble material, was resuspended by sonication in lysis buffer containing 1% SDS. The SDS content was diluted to 0.1% with lysis buffer. Total protein content was determined by Bio-Rad protein assay (Bio-Rad Laboratories, Mississauga, ON, Canada). For c-met, flag-tag and actin immunoblots, cell lysates were prepared and used for western blotting as described previously (Wiggin et al., 1998).

Results

Ectopic Pax3 induces epithelioid morphologic conversion

As part of a series of studies characterizing the interactions between cell cycle regulatory factors and proteins containing paired-like homeodomains, we characterized the consequences of ectopic Pax3 expression on specific cell lines. An N-terminal, flag-tagged version of mouse Pax3, which exhibited transcriptional and DNA-binding activities indistinguishable from wild-type Pax3 (O.W., unpublished), was expressed in the pRB-deficient human osteosarcoma cell line, Saos-2, using an adenovirus (Ad-Pax3^{flag}), which also expressed GFP. Virus expressing β -galactosidase (Ad- β gal) rather than Pax3 was used as an infection control. Following Ad- β gal or Ad-Pax3^{flag} infection at an m.o.i. of 10, 100% of Saos-2 cells became GFP positive (Fig. 1A, top panels). Immunohistochemical analysis of the Ad-Pax3^{flag}-infected cells using an α -flag antibody confirmed that all cells expressed the virally encoded Pax3^{flag} protein (data not shown). Within 48 hours postinfection, it was evident that Pax3^{flag}-expressing cells acquired a significantly altered morphology relative to control infected cells. Specifically, Ad-Pax3^{flag}-infected Saos-2 cells (Fig. 1A, right panels) assumed a more cuboidal epithelial morphology in comparison to the stellate morphology of control infected cells (Fig. 1A, left panels). Furthermore, although control infected cells are heterogeneous in size, Pax3-expressing cells were more compact relative to control cells. Morphometric distribution analysis (Table 1) showed that at 48 hours postinfection, 43% of Ad-Pax3^{flag}-infected cells had a surface area of <1000 μm^2 (average of 1162 \pm 567 μm^2) compared to control infected cells, where only 34% were <1000 μm^2 (average of 1391 \pm 758 μm^2). By 72 hours, the average cell-surface area of Ad-Pax3^{flag}-

infected cells (306 \pm 197 μm^2) was fivefold less than that of control infected cells (1478 \pm 430 μm^2). In fact, 100% of the Pax3^{flag}-expressing cells were less than 1000 μm^2 , whereas only 7% of Ad- β gal-infected cells were observed in this size range. By 72 hours postinfection, Ad-Pax3^{flag}-infected cells (Fig. 1B, right panel) were clearly morphologically distinct from control cells (Fig. 1B, left panel), appearing as multi-layered colonies of tightly aggregated cells. In a typical infection, between 70 and 80% of Ad-Pax3^{flag}-infected cells could be found in such aggregates by this time point. We noted that the induced morphological alterations were sensitive to the levels of Pax3^{flag} expressed, morphologic alterations being

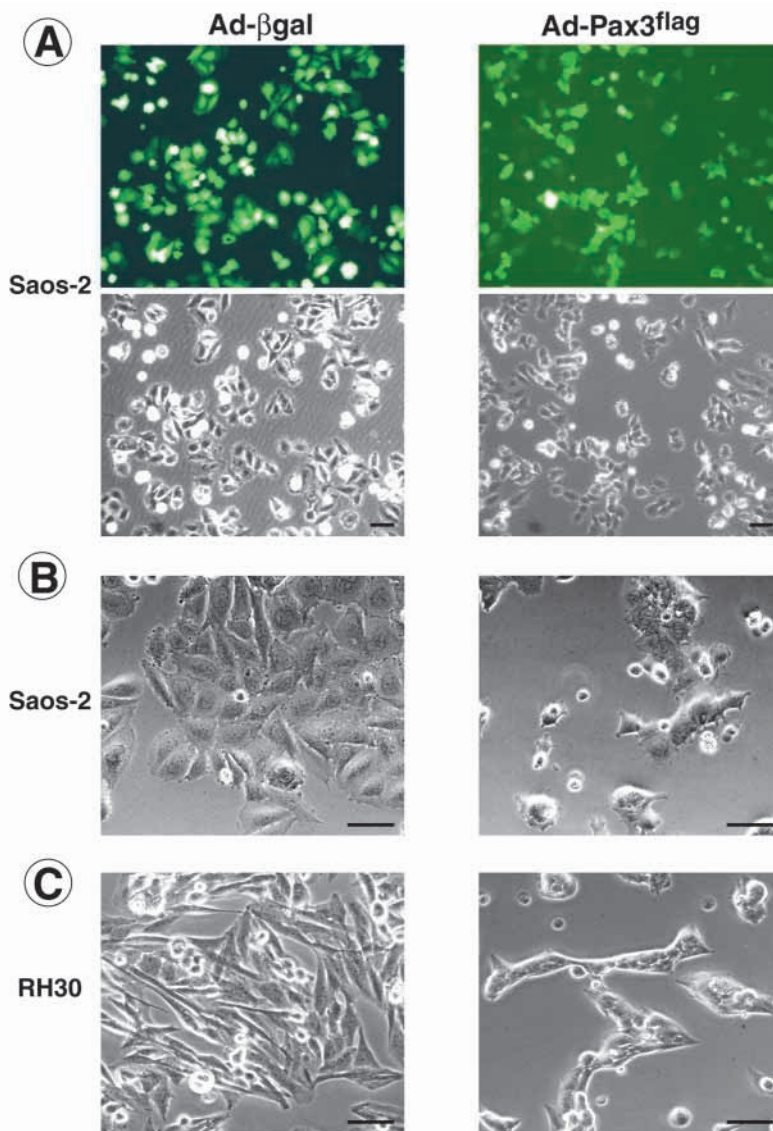


Fig. 1. Ectopic Pax3 expression induces cell aggregation and epithelioid morphologic changes in Saos-2 and Rh30 cells. Saos-2 cells were infected with adenoviruses, which simultaneously encoded GFP, in addition to either β -galactosidase (Ad- β gal) or flag-epitope tagged Pax3 (Ad-Pax3^{flag}) as indicated. At two days postinfection, GFP expression in live cells was assessed by fluorescence microscopy (A, upper panels). Phase-contrast images of the same fields are shown in A, lower panels. (B,C) Phase-contrast images of control infected and Ad-Pax3^{flag}-infected Saos-2 cells (B) and Rh30 cells (C) at three days postinfection. Bars, 80 μm .

Table 1. Ectopic Pax3 expression in Saos-2 cells results in decreased cell surface area

Surface area (μm^2)	Ad- βgal cells % (<i>n</i>)	Ad-Pax3 ^{flag} cells % (<i>n</i>)
Two days postinfection		
<1000	34 (62)	43 (84)
1001-2000	49 (89)	53 (103)
>2001	17 (30)	4 (8)
Three days postinfection		
<1000	7 (4)	100 (53)
1001-2000	80 (43)	–
>2001	13 (7)	–

Saos-2 cells were infected with Ad- βgal control or Ad-Pax3^{flag} adenovirus and the surface area of individual cells from random fields was analyzed at the indicated time points.

significantly less robust at an m.o.i of less than 5 and at m.o.i's greater than 15. The effect of Pax3^{flag} expression on cell morphology was not restricted to Saos-2 cells, which do not express endogenous Pax3 (O.W., unpublished). Ad-Pax3^{flag} infection of the rhabdomyosarcoma cell line, Rh30, which expresses the oncogenic transactivating fusion protein Pax3-FKHR (Fredericks et al., 1995), also caused formation of colonies of tightly aggregated epithelioid cells (Fig. 1C). The ability of Pax3 to induce aggregation of Rh30 cells is consistent with recent data showing that Pax3 is capable of antagonizing the activities of Pax3/FKHR and vice versa (Anderson et al., 2001).

Analysis of Saos-2 cells at three days postinfection by scanning electron microscopy revealed striking morphological changes in Ad-Pax3^{flag}-infected relative to the control infected cells (Fig. 2). Control infected cells were loosely associated and had a flattened fibroblast-like appearance (Fig. 2A,B). Membrane blebbing was frequently observed on both control infected and Ad-Pax3^{flag}-infected cells. In aggregates of Ad-Pax3^{flag}-infected cells, cells were intimately associated, having almost indiscernible cell-cell boundaries (Fig. 2C,D). In these aggregates, cells exhibited extensive membrane ruffling over their entire dorsal surface. Other distinct morphological features evident in Ad-Pax3^{flag}-infected cells relative to control infected cells included the presence of cilia of varying lengths and an apparent increase in height in these cells. Analysis of the height of individual cells by confocal microscopy revealed an average 60% increase in

the height of AdPax3-infected cells relative to control infected cells ($6.1 \pm 1.2 \mu\text{m}$, $n=30$ vs. $3.7 \pm 0.6 \mu\text{m}$, $n=30$). Together, these data show that ectopic Pax3^{flag} expression induces morphologic alterations in cultured cells, which is consistent with a mesenchymal-to-epithelial phenotypic transformation.

Epithelial junction formation of Pax3-expressing cells

The morphological changes induced by Pax3 predicted significant alterations in intercellular adhesion properties of these cells. We first assessed whether the Pax3-induced aggregation of Saos-2 cells was cadherin dependent by determining whether aggregation was Ca^{2+} dependent. Saos-2 cells, infected with Ad-Pax3^{flag}, were induced to form aggregates by maintaining them in the presence of normal Ca^{2+} -containing medium for three days (Fig. 3A). When infected cultures were then switched to low- Ca^{2+} -containing media, the Pax3-induced aggregates began dissociating within two hours. Fig. 3B illustrates that 24 hours after the switch to low- Ca^{2+} -containing media, aggregated cells had completely dispersed, supporting the notion that the Pax3-induced cell

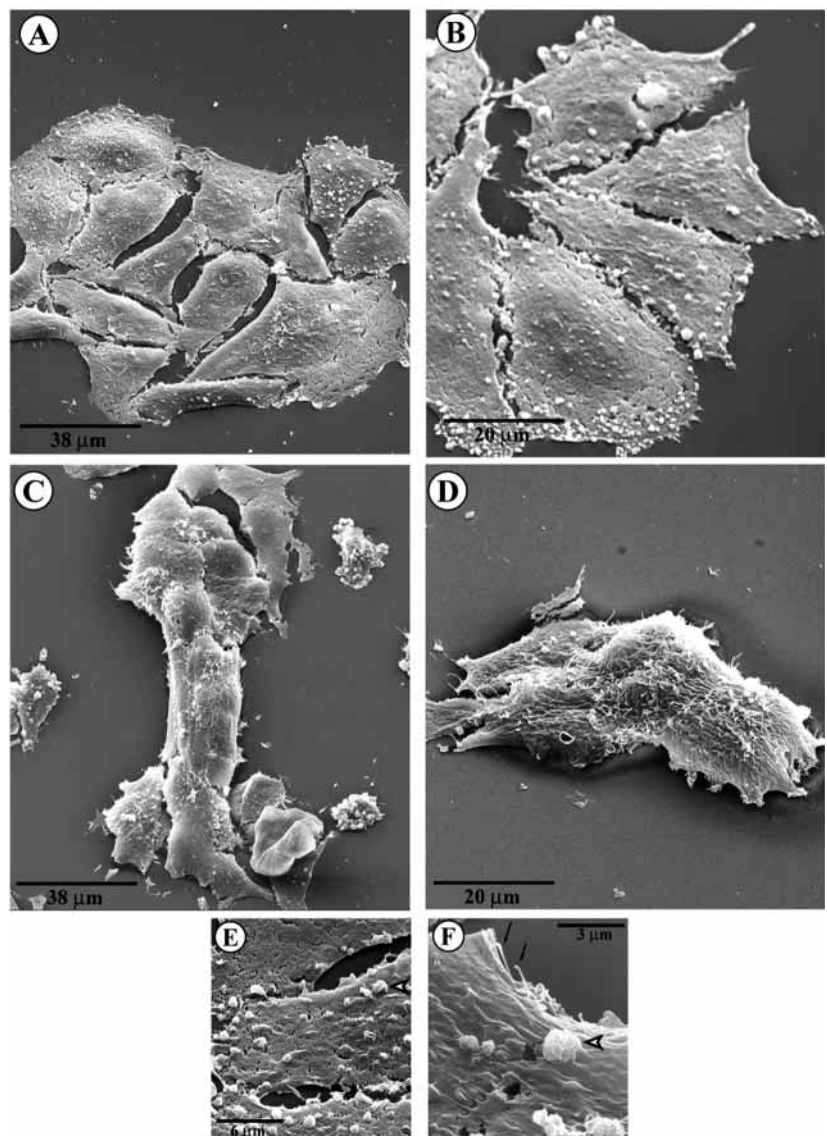


Fig. 2. Scanning electron microscopic analysis of Pax3-induced morphologic alterations in Saos-2 cells. (A–D) Scanning electron microscopic micrographs of Ad- βgal control infected (A,B) or Ad-Pax3^{flag}-infected (C,D) Saos-2 cells at three days postinfection. (E,F) Higher magnification views of the dorsal cell surface highlighting the presence of membrane blebbing (arrowheads) in both control (E) and Ad-Pax3^{flag}-infected (F) cells, as well as the presence of cilia (arrow) in Ad-Pax3^{flag}-infected cells.

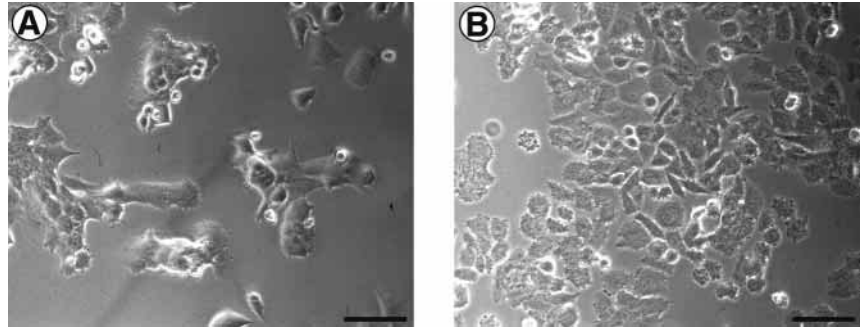


Fig. 3. Aggregation of Saos-2 cells in response to ectopic Pax3 is Ca^{2+} dependent. Phase-contrast images of live Saos-2 cells infected with Ad-Pax3^{flag} (A) in the presence of normal Ca^{2+} -containing media and cultured for three days, or (B) 24 hours after switching the media to low Ca^{2+} -containing media. Aggregates of Pax3^{flag}-expressing cells dissociated after switching to low Ca^{2+} -containing media. Bars, 80 μm .

aggregation involved the induction of Ca^{2+} -dependent, cadherin-mediated cell-cell adhesion.

Formation of epithelial type cell-cell contacts in Ad-Pax3^{flag}-infected Saos-2 cells was further characterized by examining the distribution of cadherins and cadherin-associated proteins at three days postinfection by indirect immunofluorescence. Transcripts for both an alternatively spliced version of N-cadherin (Cheng et al., 1998; Ferrari et al., 2000) and for a type II-classical cadherin expressed principally in mesenchymal tissues, cadherin-11/OB-cadherin (Cheng et al., 1998), have been detected in Saos-2 cells. Using a pan-cadherin antibody, which recognizes a common C-terminal motif present in classical cadherins, and which most likely detects a N-cadherin variant in Saos-2 cells (see below), signal was localized in Ad- β gal-infected cells to sites of intercellular cell contact in a discontinuous, punctate or serrate pattern (Fig. 4D). This staining pattern resembles that described previously for spot-adherens junctions described in nonepithelial cells (Yonemura et al., 1995). In Pax3^{flag}-expressing cells, although the pan-cadherin signal also localized to sites of cell contact (Fig. 4E), the staining pattern was distinct from control Ad- β gal-infected cells. Specifically, Pax3^{flag}-expressing cells had a continuous band of cadherin staining at sites of cell-cell contact, reminiscent of that observed at adherens junctions of epithelial cells (Yonemura et al., 1995). Moreover, cell-cell contacts were more extensive in Pax3-infected cells relative to control cells.

Using a cadherin-11-specific antibody, we observed a distinct staining pattern from that observed with pan-cadherin antibodies. In control infected cells, cadherin-11 displayed a finger-like distribution at sites of cell-cell contact (Fig. 4A). A similar distribution of cadherin-11 was observed at sites of cell-cell contact in loosely associated Ad-Pax3^{flag}-infected cells (Fig. 4B). By contrast, aggregates of Pax3^{flag}-infected cells displayed a strong reduction in cadherin-11 staining at sites of cell-cell contact (Fig. 4C). Cells in aggregates generally displayed low levels of diffuse vesicular cadherin-11 staining. Junctional and/or lateral membrane staining of cells at the margins of aggregates was frequently observed. Dual labeling of cells with both α -pan-cadherin and α -cadherin-11 antibodies revealed that the junctional signals detected by each antibody had different spatial distributions, cadherin-11 signals being typically localized more apically than those detected by pan-cadherin antibodies (data not shown).

We also characterized the subcellular distribution of α - and β -catenin; both are cadherin-associated proteins important for adherens junction formation and cytoskeletal communication. In Ad- β gal-infected cells, the pattern of α -catenin (Fig. 4F) and

β -catenin (Fig. 4G) was the same as that of pan-cadherin. Similarly, in aggregates of Pax3^{flag}-expressing cells, α -catenin (Fig. 4H) and β -catenin (Fig. 4I) formed an enriched continuous belt at sites of cell contact, a pattern identical to that of pan-cadherin and consistent with that found in epithelial cell adherens junctions.

We next examined the mechanism by which Pax3 induced increased cell adhesion in Saos-2 cells. A previous study indicated that expression of Wnt-signaling ligands may be regulated by Pax3 and other related Pax genes *in vivo* (Mansouri and Gruss, 1998). Wnts have been shown to regulate cell adhesion by regulating steady-state levels and subcellular distribution of cadherins or associated catenins, or both (Bradley et al., 1993; Hinck et al., 1994). Thus, we assessed by means of a pulse-chase assay whether expression of Pax3^{flag} affected the rate of turnover of β -catenin. As shown in Fig. 5A, no significant difference was detected in the turnover rate of β -catenin in Ad-Pax3^{flag}-infected cells relative to control cells.

Increased cell adhesion is associated with redistribution of cadherins and catenins from a cytoplasmic, detergent-soluble pool to a cytoskeleton-associated, detergent-insoluble pool (Bradley et al., 1993). Thus, we determined the subcellular distribution of cadherins and catenins by biochemical fractionation followed by western blotting (Fig. 5B). Anti-pan-cadherin antibodies detected a single band of approximately 140 kDa in cell extracts of Saos-2 cells. Anti-E- and P-cadherin antibodies failed to recognize this 140 kDa band; neither did these antibodies detect these cadherins by immunohistochemical analysis (data not shown). Although not detected by western analysis or cell staining using commercially available N-cadherin antibodies, we predict that this 140 kDa cadherin is a variant of N-cadherin based on its mass (Volk and Geiger, 1984) and the presence of N-cadherin transcripts in Saos-2 cells. The top panel in Fig. 5B illustrates the reduction ($36 \pm 6\%$) of the cadherin detected by α -pan-cadherin antibodies in the soluble fraction of Ad-Pax3^{flag}-infected cells, and its reciprocal increase in the insoluble fraction relative to control Ad- β gal-infected cells. Western blots with antibodies to cadherin-11 detected a single band of approximately 120 kDa (Fig. 5B, second panel). In contrast to the type I classical cadherin detected using the pan-cadherin antibody, Pax3^{flag}-expression caused a three-to-fourfold decrease in cadherin-11 in the detergent-soluble fraction but no commensurate increase in the insoluble fraction (Fig. 5B, second panel). Like the pan-cadherin product, β -catenin was detected in both the soluble and insoluble fractions of control and Ad-Pax3^{flag}-infected cells. Expression of Pax3^{flag} also resulted in altered distribution of β -catenin, as $28 \pm 1\%$ of total

β -catenin was found in the insoluble fraction of AdPax3^{flag}-infected cells vs. $21 \pm 1\%$ in control infected cells. A small but reproducible decrease in the apparent mass of β -catenin in the insoluble fraction of Pax3-expressing Saos-2 cells was also observed. Thus, ectopic Pax3 expression induces the formation of epithelial-type cell junctions, in part, by inducing altered subcellular distribution of cadherins and catenins.

Pax3 induces formation of epithelial apico-basal cell polarity and cytoskeletal rearrangement

One hallmark of epithelial cells is their distinct apico-basal cell polarity, these cells exhibiting distinct apical and basal structural and membrane domains (Davies and Garrod, 1997). We determined whether phenotypic epithelioid Pax3^{flag}-expressing Saos-2 cells developed apico-basal polarity by characterizing the distribution of the tight junction-associated protein, ZO-1. Optical sections through control or Ad-Pax3^{flag}-infected cells revealed the presence of ZO-1 at lateral membrane cell-cell contact sites (Fig. 6). In control infected cells, ZO-1 signal is detected throughout the entire lateral contact sites along the apico-basal axis (Fig. 6A-D,M). By contrast, in both single-layered (Fig. 6E-H,N) and multi-layered aggregates (Fig. 6I-L) of Pax3^{flag}-expressing cells, ZO-1 became concentrated at the apex of lateral cell-cell junctions. These data confirm that Pax3 induces a morphological epithelial conversion of Saos-2 cells resulting in the formation of tight junctions and cells that have acquired significant apico-basal cell polarity.

The Pax3^{flag}-induced morphological changes in Saos-2 cells led us to examine whether there were alterations to the cytoskeletal architecture. Immunofluorescence staining at three days postinfection revealed that Ad- β gal-infected cells possessed many F-actin stress fibers present throughout the cell at all levels along the apico-basal axis (Fig. 7A-D). By contrast, in aggregates of tightly associated Pax3-expressing cells, actin filaments formed distinct structures along the apico-basal axis. In these cells, thick actin bundles at the cell cortex was observed basally (Fig. 7E). Also basally, very few stress fibers were present, with actin localized to cell-cell junctions. At the level of the nucleus, strong actin staining was observed at cell-cell junctions and peripherally around the nucleus (Fig. 7F). Apically, at the submembrane cortex, actin formed wavy-like bundles that were associated with the formation of dorsal membrane ruffles in these cells (Fig. 7G).

We also examined the distribution of the cytoskeletal protein vinculin. In β gal-expressing cells, vinculin was enriched at sites of focal adhesions (Fig. 7I). In aggregates of Pax3^{flag}-expressing cells there was a significant reduction in the number of focal adhesions. In these cells, vinculin concentrated at sites of cell-cell contact, at the tips of filopodia and diffusely throughout

the cytoplasm (Fig. 7J). The presence of vinculin at sites of cell-cell contact in aggregates of Pax3^{flag}-expressing cells is consistent with the formation of epithelial-type adherens junctions (Yonemura et al., 1995).

Dramatic rearrangements to the microtubule-based cytoskeleton occurs during the formation of polarized epithelial cells (Bacallao et al., 1989; Grindstaff et al., 1998). We therefore examined microtubule organization by confocal immunohistochemical analysis with antibodies to β -tubulin. In control infected Saos-2 cells, microtubules emanate radially towards the cell periphery and run parallel to the axis of the cell substratum at all levels along the apico-basal axis (Fig. 8A-D). In aggregates of Pax3-expressing cells, a dramatic reorganization of the microtubules had occurred. Basal to the nucleus, microtubules formed a mat of criss-crossed parallel

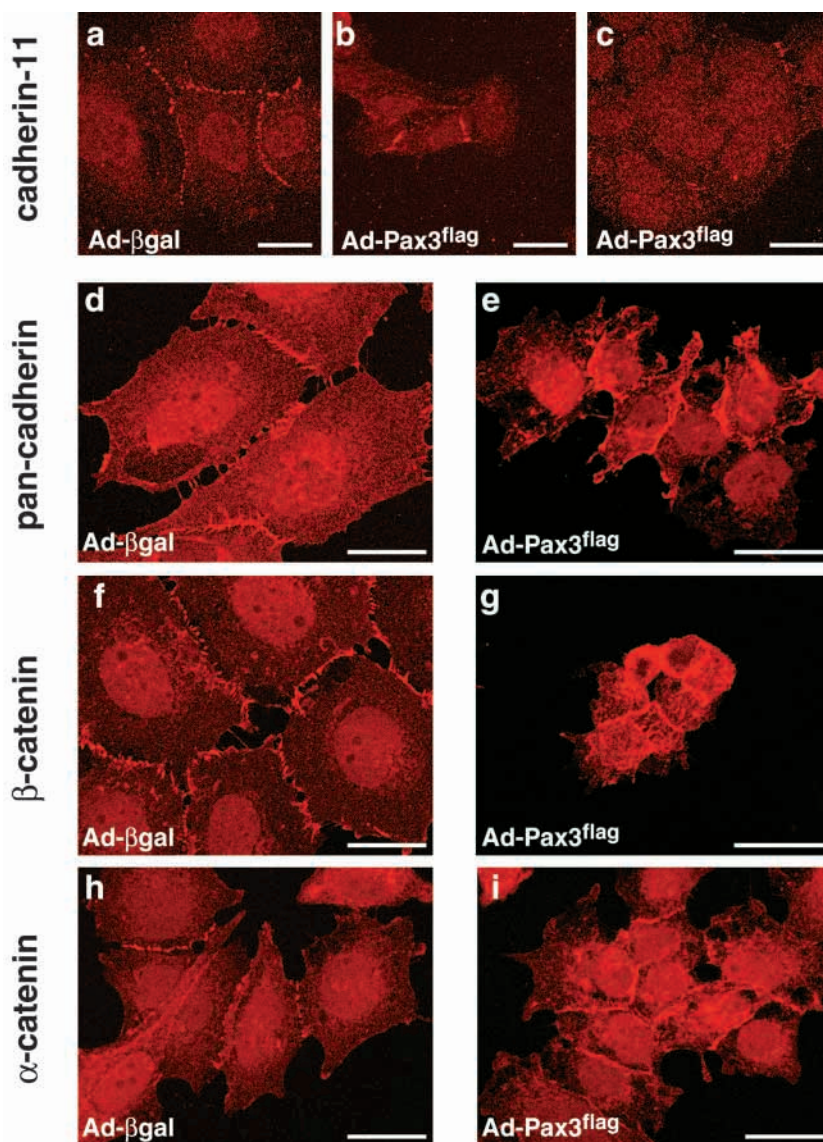


Fig. 4. Ectopic Pax3 expression induces the formation of epithelial cell-cell junctions in Saos-2 cells. Saos-2 cells were infected with either Ad- β gal control virus (a,d,f,h) or Ad-Pax3^{flag} adenovirus (b,c,e,g,i). The junctional staining of pan-cadherin (d,e), β -catenin (f,g), α -catenin (h,i) and cadherin-11 (a-c) were analyzed by indirect immunofluorescence confocal microscopy at three days postinfection. Bars, 20 μ m.

microtubules, with punctate dot-like staining also observed (Fig. 8E,I). At the level of the nucleus, β -tubulin staining was punctate, appearing as bright dots localized peripherally around the nucleus and along the lateral edges of cells (Fig. 8F,J). These punctate dots are indicative of microtubules oriented parallel to the apico-basal axis (Bacallao et al., 1989). Apically, above the level of the nucleus, microtubules also formed a dense web-like mat with many bright punctate structures (Fig. 8G,K). This organization for microtubules was observed only in aggregated Pax3^{flag}-expressing Saos-2 cells. Furthermore, this arrangement is restricted to polarized epithelial cells (Bacallao et al., 1989) and provides further evidence for a mesenchymal-to-epithelial transformation induced by Pax3 in these cells.

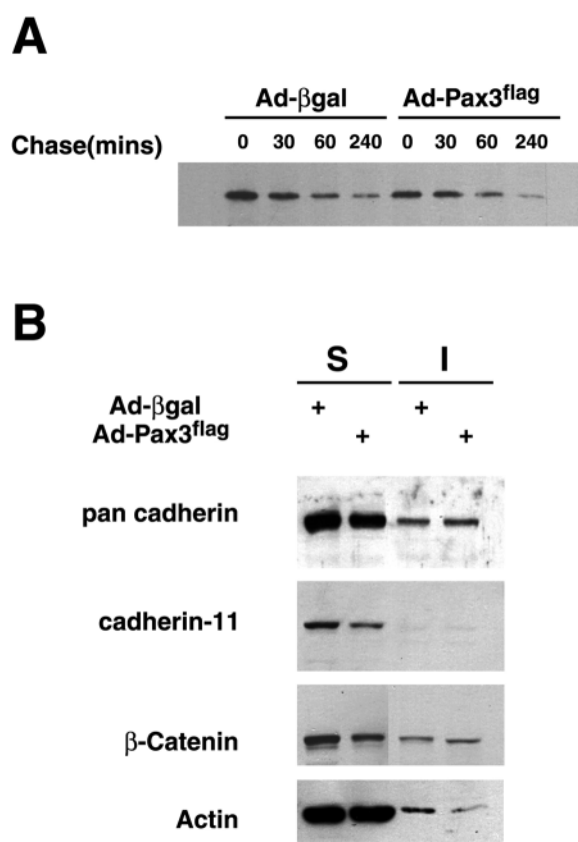


Fig. 5. Biochemical analysis of the expression and subcellular distribution of cadherins and β -catenin in response to ectopic Pax3 expression in Saos-2 cells. (A) The turnover rate of β -catenin protein was assessed by pulse-chase analysis. Control and Ad-Pax3^{flag}-infected cells were pulse labeled at three days postinfection with S³⁵ methionine and chased in the absence of label for the times indicated. Cell extracts were prepared and equivalent amounts were immunoprecipitated with antibodies directed against β -catenin. (B) The steady-state levels and distribution between the NP-40 soluble (S) and insoluble (I) fractions at three days postinfection of cadherins and β -catenin was assessed by immunoblot analysis of equivalent amounts of cell extracts of Ad- β gal- or Ad-Pax3^{flag}-infected cells. Pax3 expression resulted in altered distribution of a pan-cadherin product (B, top panel) and β -catenin (B, third panel) and in a reduction in the total levels of cadherin-11 (B, second panel). Actin immunoblot (B, bottom panel) served as a loading control.

Epithelial-to-mesenchymal phenotypic reversion in response to HGF/SF

In vertebrates, limb muscles are derived from a population of somitic cells that migrate from the lateral dermomyotome to the developing limb bud (Cossu et al., 1996). Migration requires the Pax3-dependent expression in these cells of a receptor, c-met (Bladt et al., 1995; Daston et al., 1996; Epstein et al., 1996), and expression of its ligand, HGF/SF, from cells in the proximal regions of the adjacent limb bud (Dietrich et al., 1999; Schmidt et al., 1995). HGF/SF induces dissociation of the c-met-expressing cells at lateral tips of the epithelial dermomyotome, facilitating their migration to the limb bud (Brand-Saberi et al., 1996a; Heymann et al., 1996). We determined, therefore, whether Pax3^{flag}-induced morphological changes in Saos-2 cells were accompanied by induction of c-met and whether these cells could respond to morphogenic signaling by HGF/SF. As the RT-PCR signal and western blot reveal (Fig. 9A), persistent levels of exogenous Pax3^{flag} expression caused a 1.5-to-2-fold increase of endogenous c-met transcript by 24 hours. A sevenfold increase in c-met message was detected by 72 hours. These changes in transcript levels were translated into a twofold increase of c-met protein within 48 hours and greater than fourfold by 72 hours (Fig. 9B).

We determined next whether the Pax3-dependent induction of endogenous c-met allowed Saos-2 cells to respond to HGF/SF. Six units of human HGF/SF were added to aggregated Ad-Pax3^{flag}- or control Ad- β gal-infected cells. Fig. 9D shows the complete dissociation and phenotypic epithelial-to-mesenchymal reversion of Pax3^{flag}-expressing cell aggregates within 24 hours of HGF/SF treatment (compare Fig. 9C with D). Reversion to a mesenchymal phenotype is supported by shape changes, from a cuboidal morphology to a more flattened stellate morphology, and an increase of the average cell surface area of these HGF-treated cells from 306 μm^2 to 1234 μm^2 , which was not significantly different to that of control cells. Moreover, after HGF/SF treatment, many Pax3^{flag}-expressing cells assumed an elongated motile appearance. This effect of HGF/SF was not due to the normal levels of c-met expressed in Saos-2 cells as treatment of uninfected (not shown) or Ad- β gal-infected cultures (Fig. 9E,F) with HGF/SF displayed no significant alteration of cell morphology.

Taken together, our data reveal a novel activity of Pax3 where it induces cell aggregation and a phenotypic mesenchymal-to-epithelial transition in phenotypically mesenchymal cell lines. However, Pax3 simultaneously establishes a novel cell state where these epithelialized cells can now respond to a subsequent HGF/SF-induced epithelial-to-mesenchymal transition.

Discussion

Analyses of both naturally occurring and gene-targeted mutations to vertebrate Pax genes have revealed a fundamental requirement for these transcription factors during embryogenesis (Dahl et al., 1997). However, although Pax genes play a critical role in the morphogenesis of many organs and tissues, the cellular and molecular processes regulated by Pax genes and the mechanisms by which they direct morphogenesis remain largely undefined. We showed that

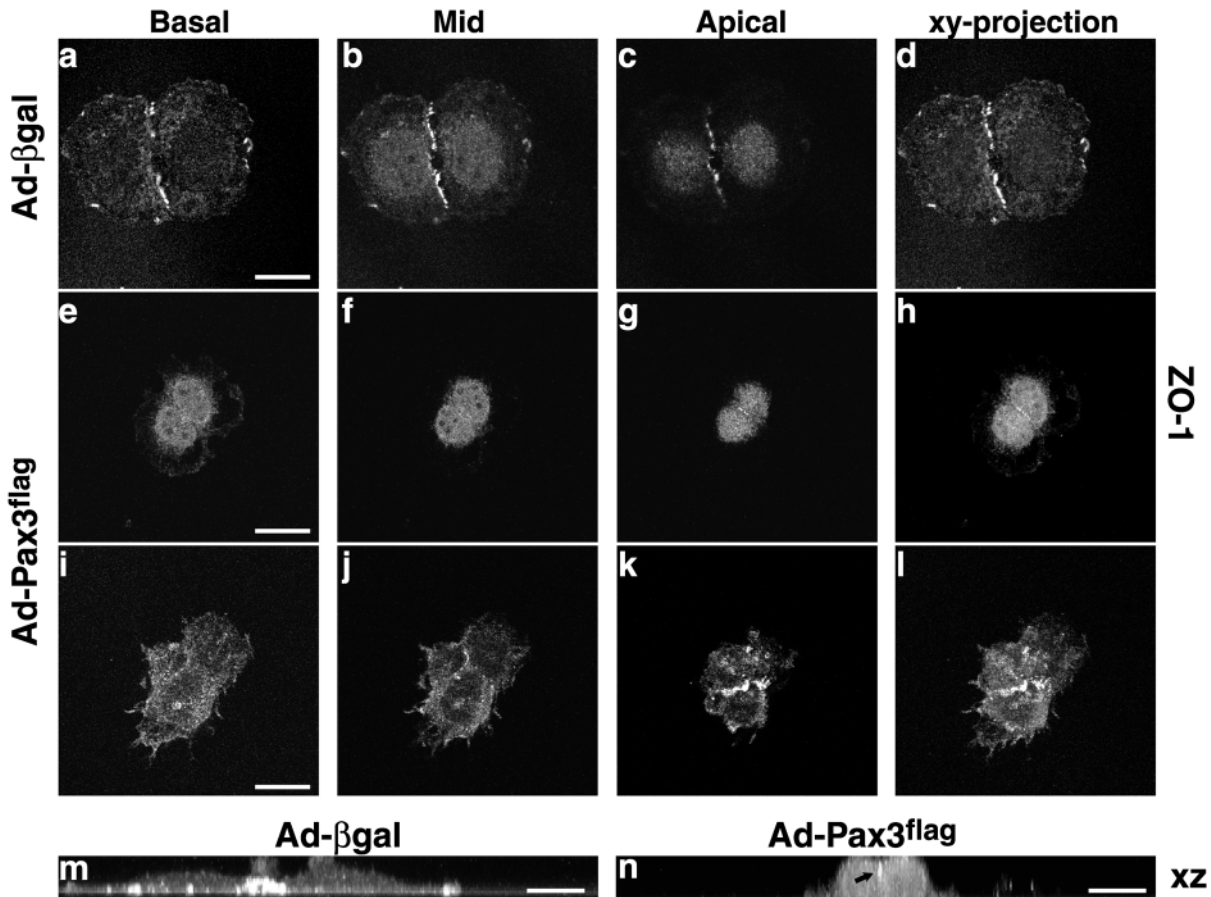


Fig. 6. Polarized distribution of the tight junction associated protein, ZO-1, in aggregates of Pax3^{flag}-expressing Saos-2 cells. The formation of apico-basal epithelial type cell polarity was assessed by examining the distribution of ZO-1 by indirect immunofluorescence confocal microscopy. The distribution of ZO-1 in control infected (a-d,m) or Ad-Pax3^{flag}-infected (e-l,n) cells was examined at three days postinfection. Optical sections through the regions indicated are depicted in a-c, e-h and i-l. Panels e-h are representative of the ZO-1 distribution in single layered aggregates, and (i-l) its distribution in multi-layered (this series depicts a two-layered aggregate) aggregates of Ad-Pax3^{flag}-infected cells. (j) Optical section through the interface between the apex of the layer of cells attached to the substratum and the basal regions of the second layer of cells. (m,n) XZ-projections of the series presented in a-d and e-f, respectively. Note that in Ad-Pax3^{flag}-infected cells, ZO-1 junctional staining is restricted to the apex of lateral sites of cell-cell contact (arrow in n), and in multi-layered aggregates the junctional staining is strongest at the apex of exposed cells (compare j and k). Bars, 20 μ m (a,e,i). Bars, 10 μ m (m,n).

ectopic Pax3 expression in at least two different mammalian cell lines induces cell aggregation and, for one of these, we further showed a mesenchymal-to-epithelial phenotypic conversion. Adenoviral-mediated, ectopic Pax3 expression in Saos-2 cells led to an increase in intercellular cell adhesion, the cells ultimately forming multi-layered condensed cell aggregates. Although ectopic Pax3 expression also induced aggregation as well as an epithelial morphology in Rh30 cells we have not yet characterized whether all of the other data presented for Saos-2 cells pertains to Rh30 cells. Aggregated Saos-2 cells displayed many epithelial characteristics, including epithelioid morphology, the presence of cilia on their apical surfaces, apico-basal polarity, epithelial-type adherens and tight junctions and epithelial-type cytoskeletal organization. Although these Pax3-induced characteristics are indicative of a mesenchymal-epithelial conversion of Saos-2 cells, our data does not preclude the possibility that these cells may not represent true epithelia. Nevertheless, as outlined below, our finding that Pax3 induces cell aggregation and imparts epithelial characteristics to cells in vitro likely mimics

these important functions for Pax3 in vivo during embryonic development. Furthermore, combined with previous studies from our lab (Wiggin et al., 1998) and from others (Epstein et al., 1996), our studies confirm *c-met* as a direct transcriptional target for Pax3 and shows, in vitro, the ability of Pax3 to program phenotypic epithelial-mesenchymal transitions in response to HGF/SF.

Our finding that Pax3 regulates cell adhesion and epithelial cell morphogenesis in vitro provides a mechanism for the developmental defects that arise when Pax3 activity or that of other Pax-family proteins is defective or absent in vivo. During vertebrate embryonic development, for example, the epithelial somite differentiates into an epithelial dermomyotome and a mesenchymal sclerotome (Brand-Saberi et al., 1996b). Pax3 is normally expressed throughout the entire epithelial dermomyotome at E9.5 of murine embryonic development. In homozygous Pax3-deficient *Splotch* (*sp*) mice, the ventrolateral aspect of the dermomyotome loses its epithelial morphology at this developmental stage (Daston et al., 1996). The medial portion of the dermomyotome in these animals

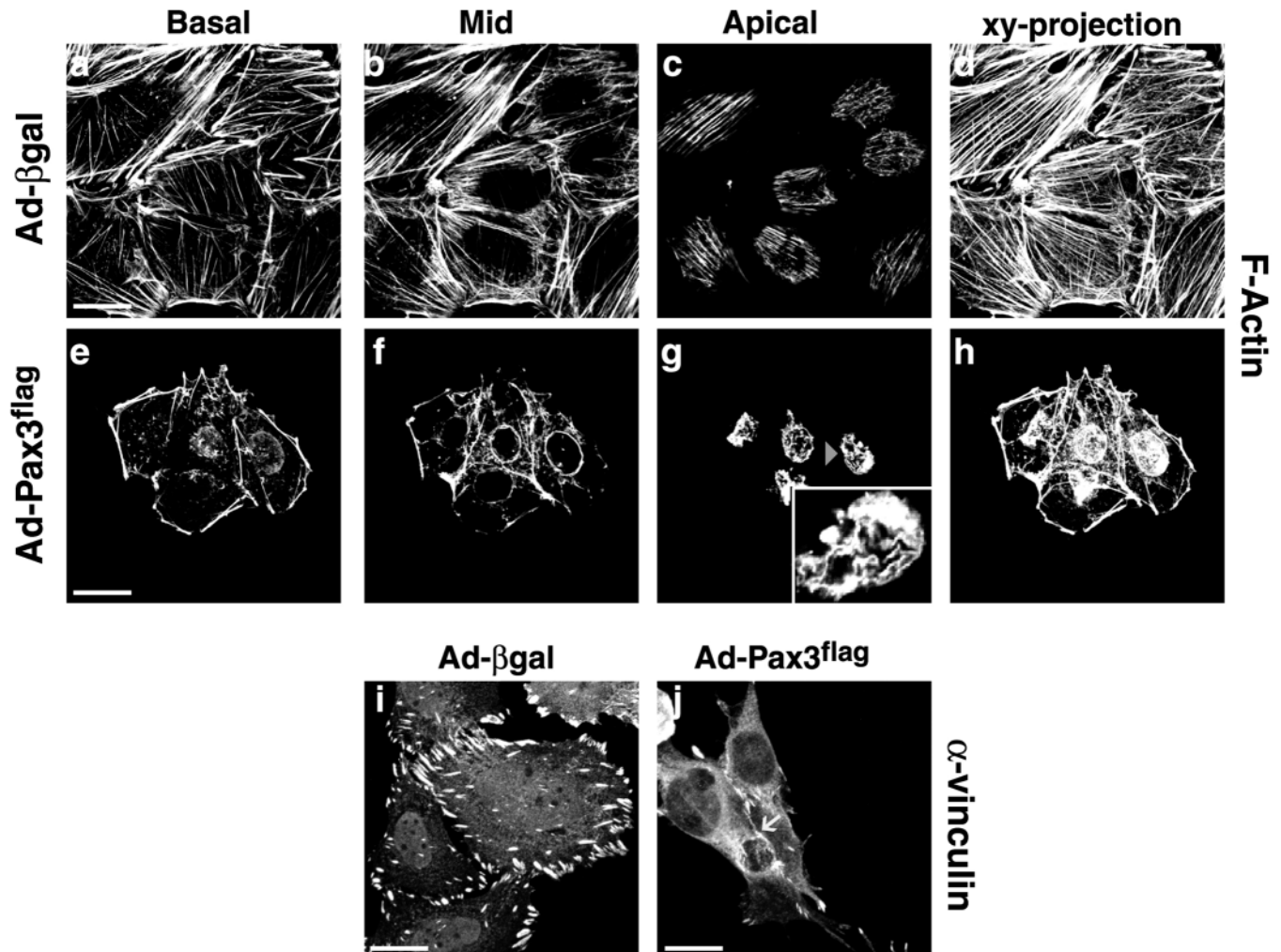


Fig. 7. Ectopic Pax3^{flag} expression induces rearrangement of actin cytoskeleton. Saos-2 cells were infected with either Ad-βgal control (a-d,i) or Ad-Pax3^{flag} (e-h,j) adenoviruses. Cytoskeleton architecture was assessed at three days postinfection by examination of the distribution of F-actin (a-h) and vinculin (i,j) by fluorescence confocal microscopy. Shown are individual optical sections captured below the level of the nucleus (a,e), at the level of the nucleus (b,f) and at the most apical regions (c,g). Projections of optical sections are shown in d and h. Inset in g is a magnified image of the cell indicated by arrowhead. In control infected cells (i), vinculin localizes to focal adhesions. In Ad-Pax3^{flag}-infected cells (j), vinculin localizes to sites of cell-cell contact (arrow), at the tips of filopodia and diffusely throughout the cytoplasm. Bars, 20 μm.

retains an epithelial morphology. This latter portion corresponds to the domain, where expression of a closely related Pax gene, *Pax7*, is maintained, indicating potential redundant activities for Pax3 and Pax7 in the maintenance of epithelial morphology of the dermomyotome (Daston et al., 1996).

Previous studies have further implicated a role for Pax3 in regulation of intercellular cell adhesion during vertebrate neurulation. During neural tube closure in normal murine development, neuroepithelial cells are tightly associated, exhibiting very little extracellular spaces. Significant intercellular spaces between neuroepithelial cells were observed, however, in the unfused neural tube of both Pax3^{sp} and Pax3^{sp^d} embryos (Morris and O'Shea, 1983; Yang and Trasler, 1991). Thus, during neural tube development, Pax3 promotes and/or maintains cadherin-mediated intercellular adhesion, as well as the epithelial architecture of neuroepithelial cells. The mechanisms by which Pax3

regulates cell adhesion and phenotypic mesenchymal-epithelial transformation are not yet clear. Wnt ligands regulate both cell adhesion (Bradley et al., 1993; Hinck et al., 1994) and mesenchymal-epithelial transitions (Kispert et al., 1998; Stark et al., 1994). In addition, the expression of distinct Wnt ligands has been shown to be regulated by Pax proteins (Kim et al., 2001; Mansouri and Gruss, 1998). Our data showed an induction in junctional cadherin and catenins following ectopic Pax3 expression. This increase was not a consequence of increased cadherin or catenin protein levels, nor was it due to stabilization of the β-catenin, as no significant change in the protein half life of β-catenin in response to Pax3 expression was observed. Rather, increased junctional cadherin and catenins was a result of redistribution of the detergent-soluble cytosolic pool of these proteins. These results are consistent with a role for Wnt activity in mediating increased cell adhesion induced by Pax3. Additionally, examination of the subcellular distribution and

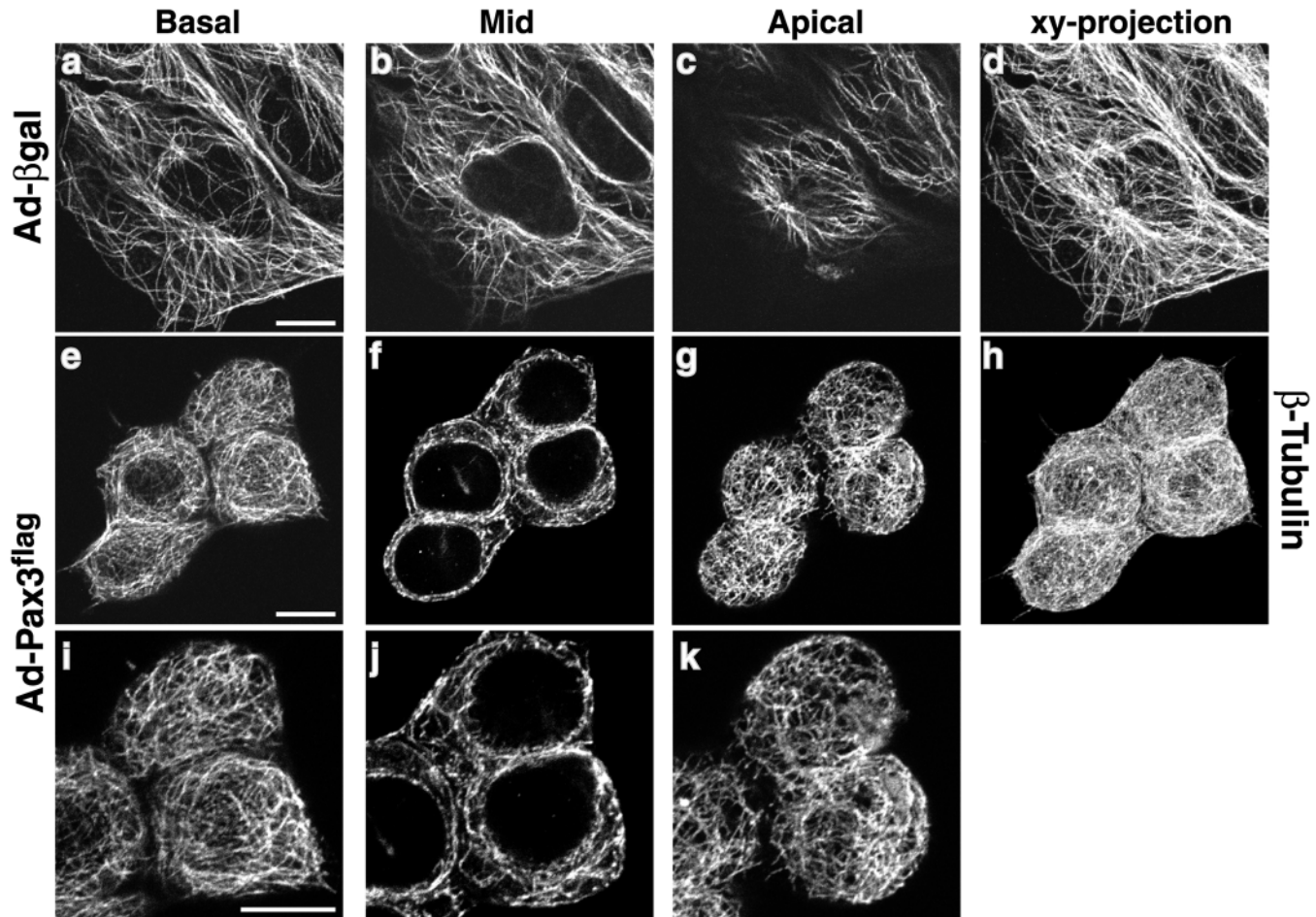


Fig. 8. Ectopic Pax3 expression induces formation of an epithelial-type microtubule organization. Saos-2 cells were infected with control (a–d) or Ad-Pax3^{flag} (e–k) adenoviruses, and microtubule organization was assessed at three days postinfection by indirect immunofluorescence confocal microscopy with antibodies to β -tubulin. Optical sections at a level below the nucleus (a,e,i), at the level of the nucleus (b,f,j) and through the apical most region (c,g,k) revealed distinct microtubule organization between Ad- β gal- and Ad-Pax3^{flag}-infected cells. Images in panels i, j and k are magnified images of e, f and g, respectively. Note the presence of many punctate dots at all levels in Ad-Pax3^{flag}-infected cells. (d,h) Projections of optical sections from each respective series. Bars, 10 μ m.

activity of both canonical and non-canonical Wnt-signaling components has provided evidence for the activation of a non-canonical Wnt-signaling cascade during Pax3 induced cell aggregation and phenotypic mesenchymal-epithelial transition (Wiggen and Hamel, 2002). Interestingly, this non-canonical Wnt signaling cascade, which entails activation of Jun-N-terminal kinase (JNK), has been implicated to regulate changes to cytoskeletal architecture and cell shape (Sokol, 2000). The dramatic Pax3-induced changes to the cytoarchitecture described herein, coupled with our finding that several components of this non-canonical Wnt-signaling cascade localize to the actin cytoskeleton, further suggests a role for Wnt activity downstream of Pax3 in mediating aspects of phenotypic mesenchymal-epithelial transition in Saos-2 cells. It remains to be determined, however, whether Pax3 regulates cell adhesion and mesenchymal-epithelial transition by inducing the expression of specific Wnt ligands.

The function of cadherin-11 in mesenchymal tissues is poorly understood. The fact that cadherin-11 is present at cell-cell junctions in loosely associated cells but its protein levels decrease during the formation of tightly aggregated

polarized cells suggests that this cadherin may be involved in the initial aggregation of cells, but may be antagonistic to the maintenance of epithelial-type cell-cell junctions. Interestingly, during similar mesenchymal-epithelial transformations that occur during both somite and kidney development, cadherin-11 is expressed in the condensed mesenchyme but is not detected in their epithelial derivatives (Hoffmann and Balling, 1995; Kimura et al., 1995; Simonneau et al., 1995).

Taken together with previous studies, our evidence for Pax3-induced formation of condensed cell aggregates in two different phenotypically mesenchymal cell lines defines an apparent common function for the Pax-family proteins. Mesenchymal condensation is initiated at the early stages of tooth, hair and kidney formation, chondrogenesis, osteogenesis and in the formation of many other organs (Thesleff et al., 1995). Mesenchymal condensation is also a pivotal early step in the mesenchymal-epithelial transitions that occur during somitogenesis and in nephrogenesis (Davies and Garrod, 1997). Our observation that ectopic Pax3 induces the formation of condensed cell aggregates and mesenchymal-epithelial

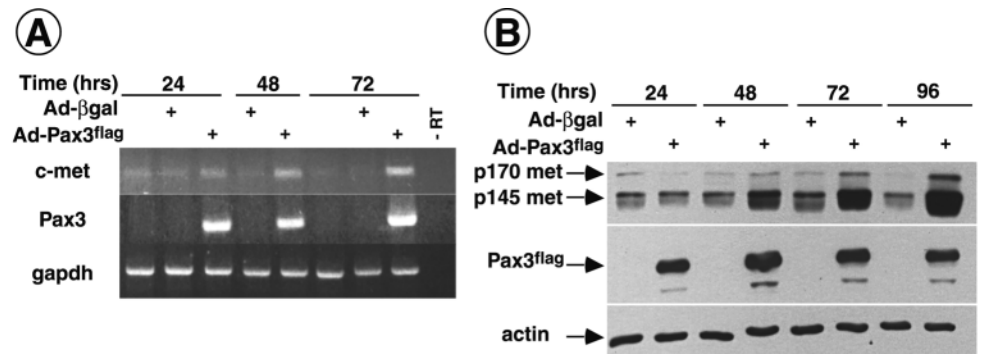
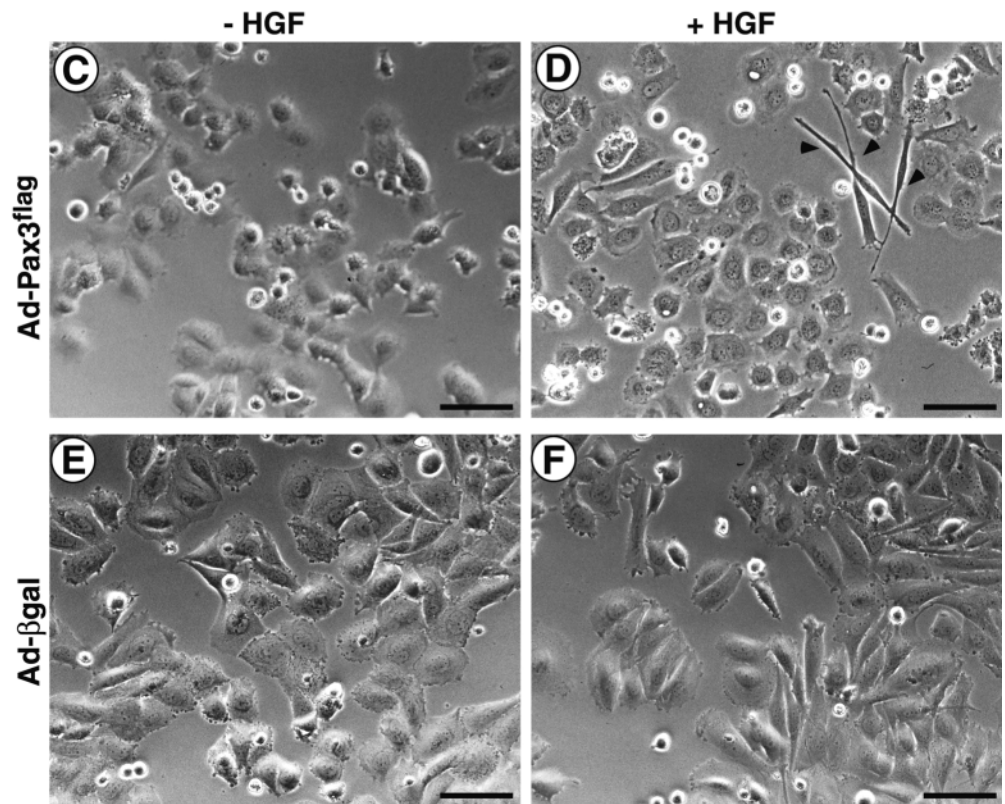


Fig. 9. Ectopic Pax3 expression induces expression of endogenous c-met and HGF induces epithelial-mesenchymal phenotypic reversion of Pax3^{flag}-expressing cell aggregates. Saos-2 cells were infected with either Ad-βgal or Ad-Pax3^{flag} viruses and harvested at the time points indicated. (A) Expression of c-met and Pax3^{flag} transcripts were assessed by semi-quantitative RT-PCR, with glyceraldehyde-3-phosphate dehydrogenase (GAPDH) from the same samples as a control. (B) Expression of c-met and Pax3^{flag} proteins was determined by western blot analysis with antibodies specific for each protein. Actin levels served as a loading control. (C-F) Phase-contrast images of Saos-2 cells infected with Ad-Pax3^{flag} (C,D) and Ad-βgal (E,F) adenovirus. At three days postinfection cells were exposed to conditioned media containing six scatter units of HGF/SF (D,F) or control conditioned media (C,E) and images of live cells were captured 24 hours later. Exposure of Ad-Pax3^{flag}-infected cells to HGF/SF led to a complete dissociation of cell aggregates with many cells exhibiting an elongated motile appearance (arrowheads in D). Bars, 80 μm.



transition suggests that Pax proteins may directly control the mesenchymal condensation process in the genesis of specific organs and tissues during development. Our studies indicate further that the initiation of mesenchymal condensations induced by Pax genes may occur, at least in part, through regulation of cell size and intercellular cell adhesion. We note that Pax3 does not induce cell aggregation in all cell types, for example fibroblasts (3T3), to the same extent as in Saos-2 and Rh30. We hypothesize that the ability of Pax3 to induce cell aggregation may depend, in part, on preexisting expression and/or sufficient levels of, for example, specific cadherins and catenins. In addition, we showed previously that the activity of Pax3 could be regulated by the pRB-family proteins (Wiggin et al., 1998). Our data here showed a significant effect of Pax3 expression on the pRB-deficient osteosarcoma line, Saos-2. By contrast, a negligible effect of Pax3 expression on the

osteosarcoma line, U2OS, which expresses a functional pRB protein, was observed (O.W., unpublished). Furthermore, inactivation in Saos-2 cells of the pRB-related factors, p107 and p130, by expression of the human papilloma virus protein E7, enhanced the ability of Pax3 to alter the Saos-2 phenotype (O.W., unpublished).

Finally, it is interesting to note that ectopic Pax3 expression did not alter cell fate along a myogenic lineage in Saos-2 cells. A previous study indicated that ectopic Pax3 expression induces myogenesis in various embryonic tissues (Maroto et al., 1997). Pax3 did not induce myogenesis in Saos-2 cells as judged by myogenin staining (data not shown). Thus, the ability of Pax3 to induce myogenesis appears to be distinct from its ability to regulate epithelial morphogenesis, the former potentially requiring the activity of distinct cell-specific cofactors.

The authors thank Sean Egan and Michal Opas for their contributions to this work. We also thank Drs Bert Vogelstein, Morag Park and Lowell Langille for providing reagents. O.W. wishes to thank Dr James Rutka for providing access to confocal imaging facility, Steven Doyle for EM work, Sabrina Noria and Sheue-Lim Meredith for assistance in obtaining reagents and Wayne Arnold for assistance with photography. This work was funded by grants to P.A.H. from the Canadian Institutes of Health Research and the National Cancer Institute of Canada with funds from the Canadian Cancer Society.

References

- Anderson, M. J., Shelton, G. D., Cavenee, W. K. and Arden, K. C. (2001). Embryonic expression of the tumor-associated PAX3-FKHR fusion protein interferes with the developmental functions of Pax3. *Proc. Natl. Acad. Sci. USA* **98**, 1589-1594.
- Atchley, W. R. and Hall, B. K. (1991). A model for development and evolution of complex morphological structures. *Biol. Rev. Camb. Philos. Soc.* **66**, 101-157.
- Auerbach, R. (1954). Analysis of the developmental effects of a lethal mutation in the house mouse. *J. Exp. Zool.* **127**, 305-329.
- Bacallao, R., Antony, C., Dotti, C., Karsenti, E., Stelzer, E. H. and Simons, K. (1989). The subcellular organization of Madin-Darby canine kidney cells during the formation of a polarized epithelium. *J. Cell Biol.* **109**, 2817-2832.
- Baldwin, C. T., Hoth, C. F., Amos, J. A., da-Silva, E. O. and Milunsky, A. (1992). An exonic mutation in the HuP2 paired domain gene causes Waardenburg's syndrome. *Nature* **355**, 637-638.
- Bladt, F., Riethmacher, D., Isenmann, S., Aguzzi, A. and Birchmeier, C. (1995). Essential role for the c-met receptor in the migration of myogenic precursor cells into the limb bud. *Nature* **376**, 768-771.
- Bradley, R. S., Cowin, P. and Brown, A. M. (1993). Expression of Wnt-1 in PC12 cells results in modulation of plakoglobin and E-cadherin and increased cellular adhesion. *J. Cell Biol.* **123**, 1857-1865.
- Brand-Saberi, B., Muller, T. S., Wilting, J., Christ, B. and Birchmeier, C. (1996a). Scatter factor/hepatocyte growth factor (SF/HGF) induces emigration of myogenic cells at interlimb level in vivo. *Dev. Biol.* **179**, 303-308.
- Brand-Saberi, B., Wilting, J., Ebensperger, C. and Christ, B. (1996b). The formation of somite compartments in the avian embryo. *Int. J. Dev. Biol.* **40**, 411-420.
- Cheng, S. L., Lecanda, F., Davidson, M. K., Warlow, P. M., Zhang, S. F., Zhang, L., Suzuki, S., St John, T. and Civitelli, R. (1998). Human osteoblasts express a repertoire of cadherins, which are critical for BMP-2-induced osteogenic differentiation. *J. Bone Miner. Res.* **13**, 633-644.
- Christ, B. and Ordahl, C. P. (1995). Early stages of chick somite development. *Anat. Embryol. (Berl.)* **191**, 381-396.
- Cossu, G., Tajbakhsh, S. and Buckingham, M. (1996). How is myogenesis initiated in the embryo? *Trends Genet.* **12**, 218-223.
- Dahl, E., Koseki, H. and Balling, R. (1997). Pax genes and organogenesis. *Bioessays* **19**, 755-765.
- Daston, G., Lamar, E., Olivier, M. and Goulding, M. (1996). Pax-3 is necessary for migration but not differentiation of limb muscle precursors in the mouse. *Development* **122**, 1017-1027.
- Davies, J. A. (1996). Mesenchyme to epithelium transition during development of the mammalian kidney tubule. *Acta Anat. (Basel)* **156**, 187-201.
- Davies, J. A. and Garrod, D. R. (1997). Molecular aspects of the epithelial phenotype. *Bioessays* **19**, 699-704.
- Dietrich, S., Abou-Rebyeh, F., Brohmann, H., Bladt, F., Sonnenberg-Riethmacher, E., Yamaai, T., Lumsden, A., Brand-Saberi, B. and Birchmeier, C. (1999). The role of SF/HGF and c-Met in the development of skeletal muscle. *Development* **126**, 1621-1629.
- Epstein, D. J., Vekemans, M. and Gros, P. (1991). Sp100 (Sp2H), a mutation affecting development of the mouse neural tube, shows a deletion within the paired homeodomain of Pax-3. *Cell* **67**, 767-774.
- Epstein, J. A., Shapiro, D. N., Cheng, J., Lam, P. Y. and Maas, R. L. (1996). Pax3 modulates expression of the c-Met receptor during limb muscle development. *Proc. Natl. Acad. Sci. USA* **93**, 4213-4218.
- Epstein, J. A., Song, B., Lakkis, M. and Wang, C. (1998). Tumor-specific PAX3-FKHR transcription factor, but not PAX3, activates the platelet-derived growth factor alpha receptor. *Mol. Cell Biol.* **18**, 4118-4130.
- Ferrari, S. L., Traianedes, K., Thorne, M., Lafage-Proust, M. H., Genever, P., Cecchini, M. G., Behar, V., Bisello, A., Chorev, M., Rosenblatt, M. et al. (2000). A role for N-cadherin in the development of the differentiated osteoblastic phenotype. *J. Bone Miner. Res.* **15**, 198-208.
- Franz, T. (1989). Persistent truncus arteriosus in the Sp100 mutant mouse. *Anat. Embryol. (Berl.)* **180**, 457-464.
- Franz, T., Kothary, R., Surani, M. A., Halata, Z. and Grim, M. (1993). The Sp100 mutation interferes with muscle development in the limbs. *Anat. Embryol. (Berl.)* **187**, 153-160.
- Fredericks, W. J., Galili, N., Mukhopadhyay, S., Rovera, G., Bencicelli, J., Barr, F. G. and Rauscher, F. J. (1995). The PAX3-FKHR fusion protein created by the t(2;13) translocation in alveolar rhabdomyosarcomas is a more potent transcriptional activator than PAX3. *Mol. Cell Biol.* **15**, 1522-1535.
- Goulding, M. D., Chalepakis, G., Deutsch, U., Erselius, J. R. and Gruss, P. (1991). Pax-3, a novel murine DNA binding protein expressed during early neurogenesis. *EMBO J.* **10**, 1135-1147.
- Grindstaff, K. K., Bacallao, R. L. and Nelson, W. J. (1998). Apiconuclear organization of microtubules does not specify protein delivery from the trans-Golgi network to different membrane domains in polarized epithelial cells. *Mol. Biol. Cell* **9**, 685-699.
- Gumbiner, B., Stevenson, B. and Grimaldi, A. (1988). The role of the cell adhesion molecule uvomorulin in the formation and maintenance of the epithelial junctional complex. *J. Cell Biol.* **107**, 1575-1587.
- Hay, E. D. (1995). An overview of epithelio-mesenchymal transformation. *Acta Anat. (Basel)* **154**, 8-20.
- He, T. C., Zhou, S., da Costa, L. T., Yu, J., Kinzler, K. W. and Vogelstein, B. (1998). A simplified system for generating recombinant adenoviruses. *Proc. Natl. Acad. Sci. USA* **95**, 2509-2514.
- Heymann, S., Koudrova, M., Arnold, H., Koster, M. and Braun, T. (1996). Regulation and function of SF/HGF during migration of limb muscle precursor cells in chicken. *Dev. Biol.* **180**, 566-578.
- Hinck, L., Nelson, W. J. and Papkoff, J. (1994). Wnt-1 modulates cell-cell adhesion in mammalian cells by stabilizing beta-catenin binding to the cell adhesion protein cadherin. *J. Cell Biol.* **124**, 729-741.
- Hoffmann, I. and Balling, R. (1995). Cloning and expression analysis of a novel mesodermally expressed cadherin. *Dev. Biol.* **169**, 337-346.
- Kim, A. S., Anderson, S. A., Rubenstein, J. L., Lowenstein, D. H. and Pleasure, S. J. (2001). Pax-6 regulates expression of SFRP-2 and Wnt-7b in the developing CNS. *J. Neurosci.* **21**, RC132.
- Kimura, Y., Matsunami, H., Inoue, T., Shimamura, K., Uchida, N., Ueno, T., Miyazaki, T. and Takeichi, M. (1995). Cadherin-11 expressed in association with mesenchymal morphogenesis in the head, somite, and limb bud of early mouse embryos. *Dev. Biol.* **169**, 347-358.
- Kispert, A., Vainio, S. and McMahon, A. P. (1998). Wnt-4 is a mesenchymal signal for epithelial transformation of metanephric mesenchyme in the developing kidney. *Development* **125**, 4225-4234.
- Mansouri, A. and Gruss, P. (1998). Pax3 and Pax7 are expressed in commissural neurons and restrict ventral neuronal identity in the spinal cord. *Mech. Dev.* **78**, 171-178.
- Maroto, M., Reshef, R., Munsterberg, A. E., Koester, S., Goulding, M. and Lassar, A. B. (1997). Ectopic Pax-3 activates MyoD and Myf-5 expression in embryonic mesoderm and neural tissue. *Cell* **89**, 139-148.
- Morris, G. L. and O'Shea, K. S. (1983). Anomalies of neuroepithelial cell associations in the Sp100 mutant embryo. *Brain Res.* **285**, 408-410.
- Munsterberg, A. E., Kitajewski, J., Bumcrot, D. A., McMahon, A. P. and Lassar, A. B. (1995). Combinatorial signaling by Sonic hedgehog and Wnt family members induces myogenic bHLH gene expression in the somite. *Genes Dev.* **9**, 2911-2922.
- Noll, M. (1993). Evolution and role of Pax genes. *Curr. Opin. Genet. Dev.* **3**, 595-605.
- Opas, M., Szweczenko-Pawlikowski, M., Jass, G. K., Mesaeli, N. and Michalak, M. (1996). Calreticulin modulates cell adhesiveness via regulation of vinculin expression. *J. Cell Biol.* **135**, 1913-1923.
- Royal, I., Lamarche-Vane, N., Lamorte, L., Kaibuchi, K. and Park, M. (2000). Activation of cdc42, rac, PAK, and rho-kinase in response to hepatocyte growth factor differentially regulates epithelial cell colony spreading and dissociation. *Mol. Biol. Cell* **11**, 1709-1725.
- Schmidt, C., Bladt, F., Goedecke, S., Brinkmann, V., Zschiesche, W., Sharpe, M., Gherardi, E. and Birchmeier, C. (1995). Scatter factor/hepatocyte growth factor is essential for liver development. *Nature* **373**, 699-702.
- Simonneau, L., Kitagawa, M., Suzuki, S. and Thiery, J. P. (1995). Cadherin 11 expression marks the mesenchymal phenotype: towards new functions for cadherins? *Cell Adhes. Commun.* **3**, 115-130.

- Sokol, S.** (2000). A role for wnts in morpho-genesis and tissue polarity. *Nat. Cell Biol.* **2**, E124-125.
- Stark, K., Vainio, S., Vassileva, G. and McMahon, A. P.** (1994). Epithelial transformation of metanephric mesenchyme in the developing kidney regulated by Wnt-4. *Nature* **372**, 679-683.
- Tajbakhsh, S., Rocancourt, D., Cossu, G. and Buckingham, M.** (1997). Redefining the genetic hierarchies controlling skeletal myogenesis: Pax-3 and Myf-5 act upstream of MyoD. *Cell* **89**, 127-138.
- Tassabehji, M., Read, A. P., Newton, V. E., Harris, R., Balling, R., Gruss, P. and Strachan, T.** (1992). Waardenburg's syndrome patients have mutations in the human homologue of the Pax-3 paired box gene. *Nature* **355**, 635-636.
- Thesleff, I., Vaahtokari, A. and Partanen, A. M.** (1995). Regulation of organogenesis. Common molecular mechanisms regulating the development of teeth and other organs. *Int. J. Dev. Biol.* **39**, 35-50.
- Torres, M., Gomez-Pardo, E., Dressler, G. R. and Gruss, P.** (1995). Pax-2 controls multiple steps of urogenital development. *Development* **121**, 4057-4065.
- Volk, T. and Geiger, B.** (1984). A 135-kd membrane protein of intercellular adherens junctions. *EMBO J.* **3**, 2249-2260.
- Walther, C., Guenet, J. L., Simon, D., Deutsch, U., Jostes, B., Goulding, M. D., Plachov, D., Balling, R. and Gruss, P.** (1991). Pax: a murine multigene family of paired box-containing genes. *Genomics* **11**, 424-434.
- Wang, Y., Goligorsky, M. S., Lin, M., Wilcox, J. N. and Marsden, P. A.** (1997). A novel, testis-specific mRNA transcript encoding an NH₂-terminal truncated nitric-oxide synthase. *J. Biol. Chem.* **272**, 11392-11401.
- Wiggan, O., Taniguchi-Sidle, A. and Hamel, P. A.** (1998). Interaction of the pRB-family proteins with factors containing paired-like homeodomains. *Oncogene* **16**, 227-236.
- Wiggan, O. and Hamel, P. A.** (2002). Pax3 regulates morphogenetic cell behavior in vitro coincident with activation of a PCP/non-canonical Wnt-signaling cascade. *J. Cell Sci.* **115**, 531-544.
- Yang, X. M. and Trasler, D. G.** (1991). Abnormalities of neural tube formation in pre-spina bifida splotch-delayed mouse embryos. *Teratology* **43**, 643-657.
- Yang, X. M., Vogan, K., Gros, P. and Park, M.** (1996). Expression of the met receptor tyrosine kinase in muscle progenitor cells in somites and limbs is absent in Splotch mice. *Development* **122**, 2163-2171.
- Yonemura, S., Itoh, M., Nagafuchi, A. and Tsukita, S.** (1995). Cell-to-cell adherens junction formation and actin filament organization: similarities and differences between non-polarized fibroblasts and polarized epithelial cells. *J. Cell Sci.* **108**, 127-142.